Southern California Earthquake Center Annual Report 2005

The transition from mainshock to aftershocks from continuous recordings of moderate earthquakes in Southern California

Zhigang Peng and John Vidale (PI)

University of California, Los Angeles

November 18, 2005

I. Scientific Accomplishments (taken mostly from *Peng et al.* [2005] and *Vidale and Shearer* [2005]).

Brief summary

One of the most fundamental questions in seismology is to understand the underlying driven forces for spatio-temporal clustering of earthquake bursts. In most cases such bursts of seismicity are understood as mainshock-aftershock triggering. However, some bursts have no clearly defined main shocks, and some have a time evolution of hypocenters that indicates the presence of aseismic processes. Our research under this project has focused on the following two directions: (1) late foreshocks and early aftershocks from continuous waveforms in Japan; (2) a survey of 71 earthquake bursts across southern California. The results from these research directions can be summarized as the follows. Typical foreshock-main shock-aftershock triggering can be mostly explained by a simple cascade of elastic stress triggering using the epidemic-type aftershock sequence (ETAS) model and the rate-and-state (RS) model. However, the swarm seismicity is likely driven by underlying geophysical disturbances such as episodic aseismic slip, or pore fluid pressure fluctuations. Our results indicate that seismic and non-seismic related stress changes share responsibility for driving the seismicity bursts in southern California.

Late foreshocks and early aftershocks from continuous waveforms in Japan

Main shock rupture is typically followed by aftershocks that diminish in rate approximately as the inverse of the elapsed time since the main shock, known as the Omori's law [*Omori*, 1894]. *Utsu et al.* [1995] introduced a modified version of the Omori's law, in which the rate $R(t) \sim 1/(t+c)^p$, with c being a constant, and p being an exponent close to 1. In addition, large earthquakes are statistically preceded by accelerating seismic activity, known as foreshocks [*Jones and Molnar,* 1979; *Abercrombie and Mori*, 1996]. Recent studies have shown that the increasing rate of foreshocks before the main shock can be described by an inverse power law with the same functional form as the modified Omori's law [*Jones and Molnar*, 1979; *Maeda*, 1999; *Helmstetter et al.*, 2003].

It is notoriously difficult to observe early aftershock activity in the noisy aftermath of large earthquakes [*Kagan*, 2004]. Many aftershocks are missing in existing catalogs in the first few minutes. Yet this period marks the transition from main shock to

aftershocks, and holds valuable information about the underlying mechanisms for earthquake triggering that control the aftershock occurrence. The seismicity rate immediately before and after a main shock is also important for short-term seismic hazard forecasting [*Gerstenberger et al.*, 2005; *Helmstetter et al.*, 2005].

We have analyzed the composite seismicity rate of ~80 M 3-5 shallow earthquake sequences in Japan from waveforms recorded by the Hi-net borehole array. By scrutinizing the high-frequency signal (Figure 1), we have detected 5 times as many aftershocks in the first 200 s as in the Japan Meteorological Agency (JMA) catalog. After correcting for the changing completeness level immediately after the main shock, we found that the aftershock rate shows a crossover from a slower decay with p = 0.5-0.6 immediately after the main shock, to a faster decay p = 0.8-0.9 at later times. In addition, the seismicity rate for the stacked foreshock sequences follows an inverse Omori's law with a p value of ~0.6-0.7 from several hundred days up to the main shock occurrence time (Figure 2).

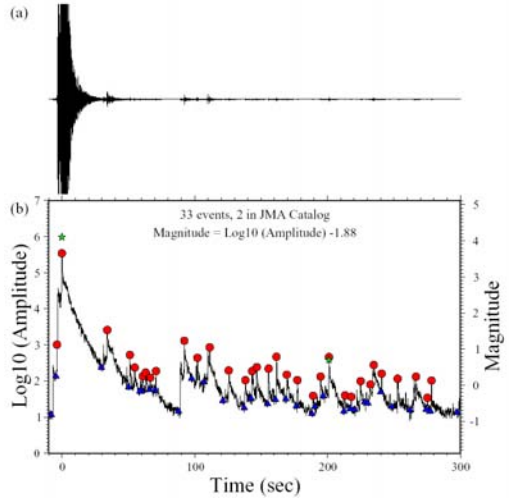

Figure 1. (a) High-pass-filtered vertical-component seismogram recorded by station KNHH for a M4.1 event. The trace is clipped, with the peak amplitude of the main shock off-scale. (b) Logarithm of the envelope function generated by stacking the envelopes of the high-pass-filtered three-component seismograms. Each red circle marks the detection of an aftershock. The green star denotes the time of two events listed in the JMA catalog. The blue triangle marks the amplitude level right before each aftershock.

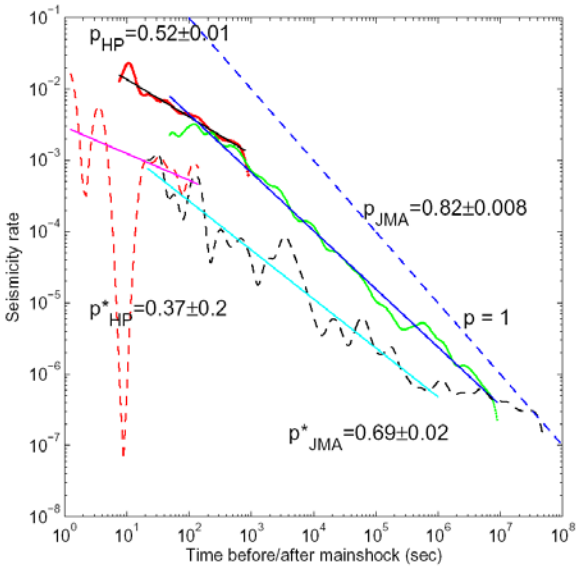

Figure 2. Aftershock seismicity rates for the 82 stacked sequences as a function of time since the main shock. The green and red lines denote the rate measured from the aftershocks in the JMA catalog, and the handpicked events after correcting for the changing completeness level immediately after the main shock. The blue and red dashed lines denote the foreshock seismicity rates from JMA catalog and handpicked events, respectively.

These observations can be explained by the epidemic-type aftershock sequence (ETAS) model [*Kagan and Knopoff*, 1981; *Ogata*, 1988; *Helmstetter and Sornette*, 2002], and by the rate-and-state (RS) model [*Dieterich*, 1994; *Ziv*, 2003; *Helmstetter and Shaw*, 2005]. However, the foreshock activity in the last 200 s before the main shock is significantly different from the long-

term foreshock increasing rates, suggests that other non-seismic stress changes near the source region, such as episodic aseismic slip, or pore fluid pressure fluctuations, may be partially responsible for driving the earthquake sequences.

A survey of 71 earthquake bursts across southern California

In this direction (2) of our research, we investigated the cause of seismicity swarms by examining a waveform-relocated catalog [*Shearer et al.*, 2005] for southern California between 1984 and 2002. We systematically identified 71 isolated sequences of 40 or more earthquakes occurring within a 2-km-radius volume and a four-week interval (Figure 3). 57 of the 71 bursts are difficult to interpret as primarily a mainshock and its Omori-law-abiding foreshocks and aftershocks because they exhibit a more complicated evolution in space, time, and magnitude; we identify 18 of these sequences as particularly swarm-like.

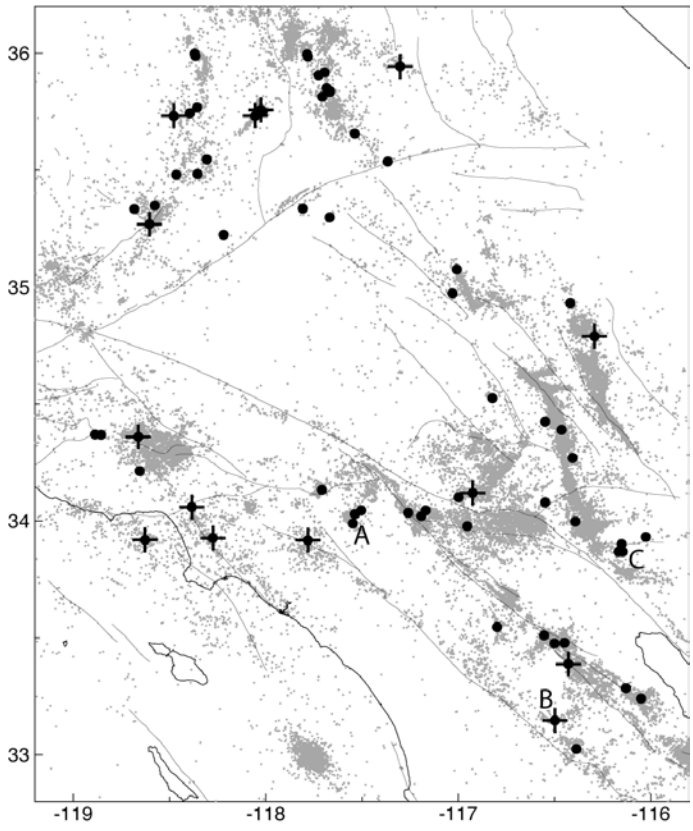

Figure 3. Locations of the 71 earthquake clusters in southern California (black dots), together with 1984 to 2002 seismicity from the SHLK_1.01 catalog (gray dots) and active Quaternary faults (thin lines). The 14 clusters marked with the crosses began with their largest event and so resemble traditional mainshocks with aftershocks.

Evidence against a simple cascade of elastic stress triggering includes the presence of an interval of steady seismicity rate (Figure 4), the tendency of the largest event to strike later in the sequence, the large spatial extent of some of the swarms compared to their cumulative moment, and the weak correlation between the number of events in each burst and the magnitude of the largest event in each burst (Figure 5).

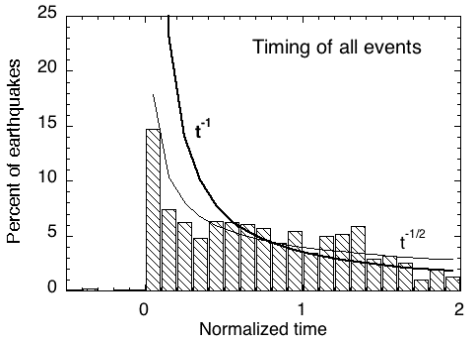

Figure 4. Rate of seismicity as a function of time after swarm initiation divided by the mean time over the entire swarm since initiation. The 57 swarms that do not start with their largest event are plotted.

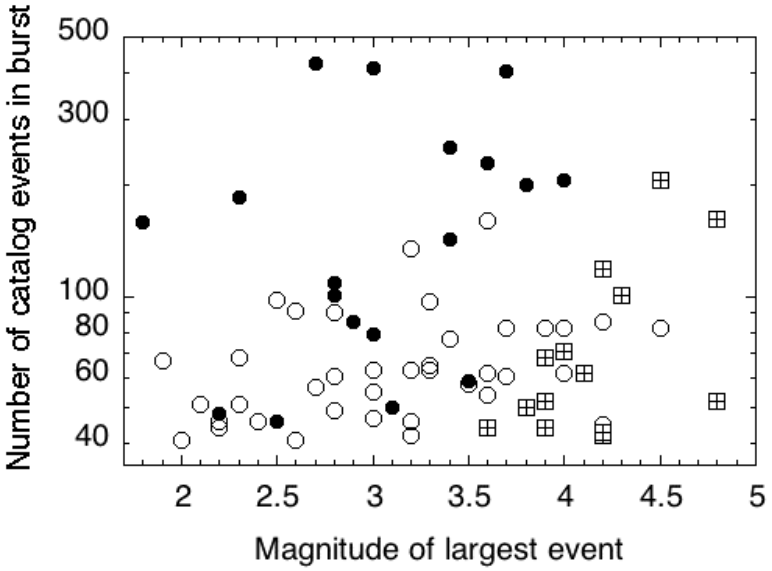

Figure 5. A comparison between the total number of events and the magnitude of the largest event in the 71 seismicity bursts. There is no tendency for larger mainshocks to generate sequences with more events. The 14 bursts in which the largest event is the initiating event are marked by crossed squares, the 18 most swarm-like by filled circles, and rest by hollow circles.

In addition, shallow sequences and normal-faulting-mechanism sequences are most likely to be swarm-like. The tendencies of the hypocenters in the swarm-like sequences to occur on vertical planes and expand over time suggest pore fluid pressure fluctuations [e.g., *Ake et al.*, 2005] as the most likely mechanism driving the swarm-like seismicity bursts (Figure 6). However, episodic aseismic slip [*Linde et al.*, 1996, *Nadeau and McEvilly*, 2004, *McGuire et al.*, 2005] could also be at least partly responsible, and might provide a more compelling explanation for the steady rate of seismicity during swarms, whereas fluid pressure perturbations might be expected to diminish more rapidly with time. Both aftershock-like and swarm-like seismicity bursts are distributed across the entire study region (Figure 3), indicating that they are a general feature of tectonic faulting, rather than limited to a few geological conditions such as volcanic or geothermal areas [*Benoit and McNutt*, 1996].

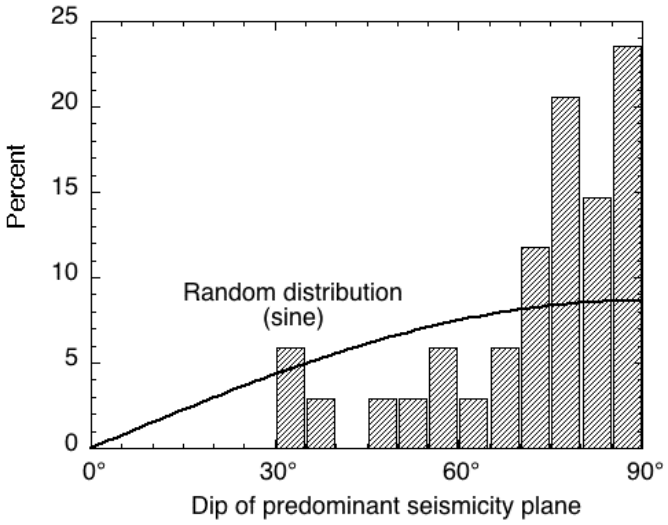

Figure 6. Distribution of seismicity-plane dip angles in the 34 seismicity bursts with planarity above 0.82. Bursts that are most planar and shallow are particularly concentrated at steep dips. A uniform distribution of fault-normal vectors would have a density of dip angles following the sin of the dip angle.

References

Ake, J., K. Mahrer, D. O'Connell, and L. Block (2005), Deep-injection and closely monitored induced seismicity at Paradox Valley, Colorado, *Bull. Seism. Soc. Am.*, *95*, 664-683.

Abercrombie, R.E. and J. Mori (1996), Occurrence patterns of foreshocks to large earthquakes in the western United States, *Nature*, *381*, 303–307.

Benoit, J.P., and S.R. McNutt (1996), Global volcanic earthquake swarm database 1979-1989, in *Open-file report 96-69, edited by USGS*, pp. 333.

Dieterich, J. H. (1994), A constitutive law for rate of earthquake production and its application to earthquake clustering, *J. geophys. Res.*, *99*, 2601–2618.

Gerstenberger, M. C., S. Wiemer, L. M. Jones and P. A. Reasenberg (2005), Real-time forecasts of tomorrow's earthquakes in California, *Nature*, *435*, 328–331, doi:10.1038/nature03622.

Helmstetter, A., and D. Sornette (2002), Subcritical and supercritical regimes in epidemic models of earthquake aftershocks, *J. Geophys. Res.*, *107*(B10), 2237, doi:10.1029/2001JB001580.

Helmstetter, A., and B. E. Shaw (2005). Estimating stress heterogeneity from aftershock rate, submitted to *J. Geophys. Res.* (http://www.arxiv.org/abs/physics/0509252).

Helmstetter, A., D. Sornette, and J.-R. Grasso (2003), Mainshocks are aftershocks of conditional foreshocks: How do foreshock statistical properties emerge from aftershock laws, *J. Geophys. Res.*, *108*, 2046, doi:10.1029/2002JB001991.

Helmstetter, A., Y. Kagan and D. Jackson, (2005), Importance of small earthquakes for stress transfers and earthquake triggering, *J. Geophys. Res.*, *110*, B05S08, 10.1029/2004JB003286.

Jones, L. M., and P. Molnar (1979), Some characteristics of foreshocks and their possible relationship to earthquake prediction and premonitory slip on fault, *J. Geophy. Res.*, *84*, 3596–3608.

Kagan, Y. Y. (2004), Short-term properties of earthquake catalogs and models of earthquake source, *Bull. Seismol. Soc. Am.*, *94*(4), 1207–1228.

Kagan, Y. Y., and L. Knopoff (1981), Stochastic synthesis of earthquake catalogs, *J. Geophys. Res.*, *86*, 2853–2862.

Linde, A.T., M.T. Gladwin, M.J.S. Johnston, R.L. Gwyther, and R.G. Bilham (1996), A slow earthquake sequence on the San Andreas fault, *Nature*, *383*, 65-68.

Maeda, K. (1999), Time distribution of immediate foreshocks obtained by a stacking method, *Pure Appl. Geophy.*, *155*, 381–394.

McGuire, J.J., M.S. Boettcher, and T.H. Jordan (2005), Foreshock sequences and short-term earthquake predictability on East Pacific Rise transform faults, *Nature*, *434* (7032), 457-461.

Nadeau, R.M., and T.V. McEvilly (2004), Periodic pulsing of characteristic microearthquakes on the San Andreas Fault, *Science*, *303* (5655), 220-222.

Ogata, Y. (1988), Statistical models for earthquake occurrence and residual analysis for point processes, *J. Am. Stat. Assoc.*, *83*, 9–27.

Omori, F. (1894). On the after-shocks of earthquakes, *J. College Sci. Imp. Univ. Tokyo*, 7, 111–200, 1894.

Peng, Z., J.E. Vidale, M. Ishii, A. Helmstetter (2005). Seismicity rates immediately before and after main shock, *J. Geophys. Res.*, to be submitted.

Shearer, P.M., E. Hauksson, and G. Lin (2005), Southern California hypocenter relocation with waveform cross-correlation: Part 2. Results using source-specific station terms and cluster analysis, *Bull. Seism. Soc. Am.*, 95, 904–915.

Utsu, T., Y. Ogata, and R.S. Matsu'ura (1995), The centenary of the Omori formula for a decay law of aftershock activity, *J. Phys. Earth*, 43, 1–33.

Vidale, J. E., and P. M. Shearer (2005), A survey of 71 earthquake bursts across southern California: Exploring the role of pore fluid pressure fluctuations and aseismic slip as drivers, submitted to *J. Geophys. Res.*

Ziv, A (2003), Foreshocks, aftershocks, and remote triggering in quasi-static fault models, *J. Geophys. Res.*, 108, 2498, doi:10.1029/2002JB002318.

II. Outreach Accomplishments.

A. The results obtained in this project were published in two papers and presented in the 2005 annual meetings of the Seismological Society of America, SCEC, and American Geophysical Union, and several Seismology seminars in USC, UCSD, and USGS Melno Park.

B. The computer codes developed in identifying earthquake swarms are now used by two undergraduate students (Clara Yoon and Katie Boyle) at UCLA to study swarm activities in northern California and Japan.

C. A list of SCEC-supported publications that are not already in the SCEC publication database.

Peng, Z., J.E. Vidale, M. Ishii, A. Helmstetter (2005). Seismicity rates immediately before and after main shock, *J. Geophys. Res.*, to be submitted.

Vidale, J. E., and P. M. Shearer (2005), A survey of 71 earthquake bursts across southern California: Exploring the role of pore fluid pressure fluctuations and aseismic slip as drivers, submitted to *J. Geophys. Res.*

III. Appendices.

A. Funding from this project has partially supported the postdoctoral work of Zhigang Peng at UCLA.